Cage Rotor MMF: Winding Function Approach

G. Joksimovic, M. Djurovic, J. Penman

Author Affiliation: Department of Electrical Engineering, University of Montenegro, Montenegro, Yugoslavia; Department of Engineering, University of Aberdeen, Scotland, U.K.

Abstract: An analytical expression for the cage rotor magnetomotive force (MMF) is derived using the winding function approach. This approach enables the analysis of stator current spectra in the cage rotor induction machine. It is demonstrated that in stator current spectra one can observe only harmonic components at high frequencies, known as the rotor slot harmonics. The position of these components in stator current spectra depends on the number of rotor bars, number of poles of the induction machine, and slip (i.e., on the actual speed of rotor).

Keywords: Induction motor, MMF, cage rotor, rotor slot harmonics, winding function.

Introduction: A noninvasive technique used often for condition monitoring of cage rotor induction machines is current signature analysis. This method is based on the monitoring of the stator current spectra in real time. The appearance of stator current components or increase of magnitude of some components at characteristic frequencies indicates a fault condition in a machine. These characteristic frequencies for common faults in cage rotor machines such as broken rotor bar(s), static or dynamic eccentricity, etc., are widely known in the literature [1]. On the other hand, the rotor slot harmonics, whose position in the stator current spectra depends on actual rotor speed, have found application in modern speed detection techniques [2].

In this letter an analytical equation is derived for the cage rotor MMF by using the winding function approach, [3]. In addition, the stator current spectrum in the cage rotor induction machine is analyzed in relation to the nature of cage rotor MMF.

MMF of Symmetrical Three-Phase Stator Winding: The equation for this MMF is known to be [4]

$$M_s(t,\theta)=\sum_{\mu} M_{s\mu}\cos(\omega_1 t-\mu p\theta);\quad \mu=6g+1;\quad g=0,\pm1,\pm2,... \tag{1}$$

where p is the number of pole pairs and $M_{s\mu}$ is amplitude of the μ^{th} harmonic. It is clear that beside the fundamental MMF wave ($g=0,\mu=1$) there exist waves with $5p$, $7p$, $11p$, $13p$, ... pair of poles, even in the case of symmetrical machines. By assuming uniform air-gap length, the flux density waves in the air-gap produced by stator windings will be of the same waveform.

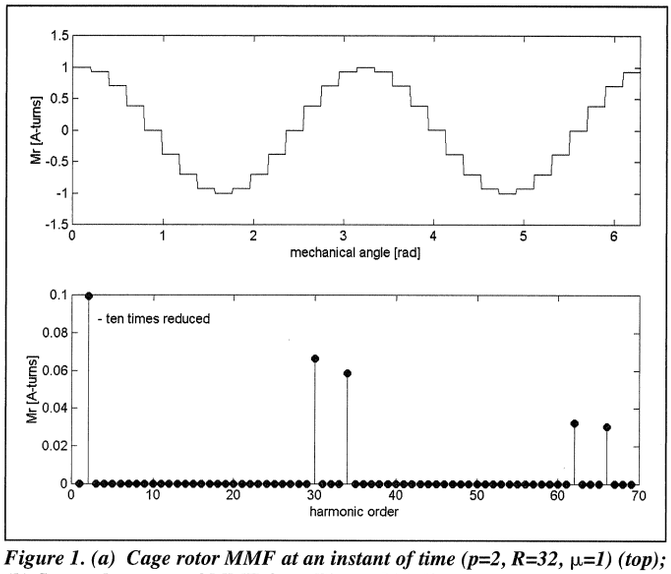

Figure 1. (a) Cage rotor MMF at an instant of time (p=2, R=32, μ=1) (top); (b) Spectral content of MMF from Figure 1(a) (bottom)

Cage Rotor MMF: The winding functions of multiturn coils placed in the slots described by angular coordinates 1 and 2 are defined by

$$N(\theta)=\begin{cases} N\cdot\left(1-\dfrac{\alpha}{2\pi}\right), & \theta_1\le\theta\le\theta_2 \\ -N\cdot\dfrac{\alpha}{2\pi}, & \text{for rest of } \theta \end{cases} \tag{2}$$

where N is the number of turns and α is a coil pitch, $\alpha=\theta_2-\theta_1$. Two near-by bars and ring segments between them make the rotor loop. Therefore, the rotor loop can be observed as a one-turn coil with pitch $\alpha=2\pi/R$, where R is the number of rotor bars. Hence, the winding function of the rotor loop 1, whose magnetic axis is in the center of the reference frame fixed to the rotor, is given by

$$N_{\text{loop1}}(\theta_r)=\begin{cases} \left(1-\dfrac{1}{R}\right), & -\dfrac{\pi}{R}\le\theta_r\le\dfrac{\pi}{R} \\ -\dfrac{1}{R}, & \text{for rest of } \theta_r. \end{cases} \tag{3}$$

This function can be resolved in Fourier series as follows:

$$N_{\text{loop1}}(\theta_r)=\sum_{\nu=1}^{\infty}\frac{2}{\nu\pi}\sin\left(\nu\frac{\pi}{R}\right)\cos(\nu\theta_r). \tag{4}$$

The rotor current, which flows in this loop as a result of μ^{th} stator flux density space harmonic, produces the following MMF:

$$M_{\text{loop1}}(t,\theta_r)=\sum_{\nu=1}^{\infty}\frac{2}{\nu\pi}\sin\left(\nu\frac{\pi}{R}\right)I_{r\mu m}\cos(s_\mu\omega_1 t)\cos(\nu\theta_r) \tag{5}$$

where $s_\mu=1-\mu(1-s)$, and s is the slip. Equation (5) can be resolved as

$$M_{\text{loop1}}(t,\theta_r)=\sum_{\nu=1}^{\infty}K_{\mu\nu}\left[\cos(s_\mu\omega_1 t+\nu\theta_r)+\cos(s_\mu\omega_1 t-\nu\theta_r)\right]. \tag{6}$$

In the next rotor loop, which is in space displaced for $2\pi/R$, flows current of the same magnitude and frequency but shifted in phase by $\mu\cdot p\cdot 2\pi/R$. This rotor loop produces MMF

$$M_{\text{loop2}}(t,\theta_r)=\sum_{\nu=1}^{\infty}K_{\mu\nu}\left[\cos\left(s_\mu\omega_1 t+\nu\theta_r-(\nu+\mu p)\frac{2\pi}{R}\right)+\cos\left(s_\mu\omega_1 t-\nu\theta_r+(\nu-\mu p)\frac{2\pi}{R}\right)\right]. \tag{7}$$

It can be shown that by summing MMFs of all rotors loops that the resultant MMF of the cage rotor is

$$M_r(t,\theta_r)=\sum_{i=0}^{R-1}\sum_{\nu=1}^{\infty}K_{\mu\nu}\left[\cos\left(s_\mu\omega_1 t+\nu\theta_r-i\cdot(\nu+\mu p)\frac{2\pi}{R}\right)+\cos\left(s_\mu\omega_1 t-\nu\theta_r+i\cdot(\nu-\mu p)\frac{2\pi}{R}\right)\right]. \tag{8}$$

Discussion: The case when rotor currents are due to μ^{th} stator flux density space harmonic is considered. By inspection of (8), the following rotor MMF waves exist: for $\nu=\pm\mu p$ as well as for $\nu+\mu p=\pm\lambda R$ and $\nu-\mu p=\pm\lambda R$, i.e., for $\nu=\pm\lambda R-\mu p$ and $\nu=\pm\lambda R+\mu p$, where $\lambda=1,2,3...$ Since ν can be only a positive integer, it follows that the cage rotor MMF waves exist only for $\nu=|\mu|p$, $\nu=|\lambda R+\pi p|$, and $\nu=|\lambda R-\mu p|$. Therefore, in addition to the fundamental cage rotor MMF wave ($\nu=|\mu|p$), which is the armature reaction on the stator MMF wave, there is also the so-called rotor slot harmonics of order $|\lambda R\pm\mu p|$, $\lambda=1,2,3...$ These harmonics are the direct consequence of the space distribution of rotor bars, i.e., of placement of rotor cage in

slots. Therefore, the rotor currents caused by the μth stator flux density space harmonic produce the following MMF waves:

$$M_{r\mu}(t,\theta_r) = M_{r\mu 1}(t,\theta_r) + M_{r\mu sh1}(t,\theta_r) + M_{r\mu sh2}(t,\theta_r) \quad (9)$$

where

$$M_{r\mu 1}(t,\theta_r) = M_{r\mu 1}\cos(s_\mu \omega_1 t - \mu p\theta_r) \quad (10)$$

$$M_{r\mu sh1}(t,\theta_r) = M_{r\mu sh1}\cos(s_\mu \omega_1 t + (\lambda R - \mu p)\theta_r) \quad (11)$$

$$M_{r\mu sh2}(t,\theta_r) = M_{r\mu sh2}\cos(s_\mu \omega_1 t - (\lambda R + \mu p)\theta_r) \quad (12)$$

or, observed from the stator side, using transformation $\theta = \theta_r + \omega_1 t\cdot((1-s)/p)$,

$$M_{r\mu 1}(t,\theta) = M_{r\mu 1}\cos(\omega_1 t - \mu p\theta) \quad (13)$$

$$M_{r\mu sh1}(t,\theta) = M_{r\mu sh1}\cos\left(\left(1-\frac{\lambda R}{p}(1-s)\right)\omega_1 t + (\lambda R - \mu p)\theta\right) \quad (14)$$

$$M_{r\mu sh2}(t,\theta) = M_{r\mu sh2}\cos\left(\left(1+\frac{\lambda R}{p}(1-s)\right)\omega_1 t - (\lambda R + \mu p)\theta\right). \quad (15)$$

Figure 1(a) shows the waveform of the fundamental cage rotor MMF wave ($\mu = 1$) at a time instant assuming that the amplitude of the rotor loop current is 1A. Rotor has $R = 32$ bars and it is assumed that machine has two pair of poles, $p = 2$. Figure 1(b) shows spectral contents of MMF wave from Figure 1(a). It is obvious that beside fundamental harmonic ($\mu p = 2^{nd}$), there exist rotor slot harmonics, $R-p$ and $R+p$, $2R-p$ and $2R+p$, etc. (i.e., 30th, 34th, 62nd, 66th). This follows from (11) and (12).

Figure 2(a) shows the waveform of the cage rotor MMF, produced by rotor currents that are the result of $\mu = -5$ stator flux density space harmonic for the same machine and, once again, under assumption that the amplitude of rotor loop current is 1 A. In this case, the number of rotor bars per one pole of harmonic field is less than before, so as a result, more rugged waveform is obtained.

The spectral content of the waveform from Figure 2(a) is shown in Figure 2(b). It is obvious that in addition to the "fundamental" harmonic (now, MP=10th), the rotor slot harmonics of the order (R–5·p), (R+5·p), (2R–5·p), (2R+5·p), i.e., 22nd, 42nd, 54th, 74th will appear. It is in accordance with (11) and (12) as well. It is obvious that now the amplitude of rotor slot harmonics are more pronounced relative to the "fundamental" harmonic when compared to the situation in Figure 1(b).

However, the main conclusion can be derived from (13), (14), and (15). The cage rotor of induction machine reflects all MMF space harmonics from stator side at the fundamental frequency (f_1) and at frequencies $(1 \pm \lambda R(1-s)/p)f_1$. By taking into account only the constant term of permeance of the air-gap in induction machines, the flux density waves will have the same form as MMF waves. Thus, the induced emfs, as well as currents, in a stator winding can be expected to appear at discussed frequencies. The magnitudes of these emfs (currents) depend on the number of pole pairs of the reflected flux density waves. It

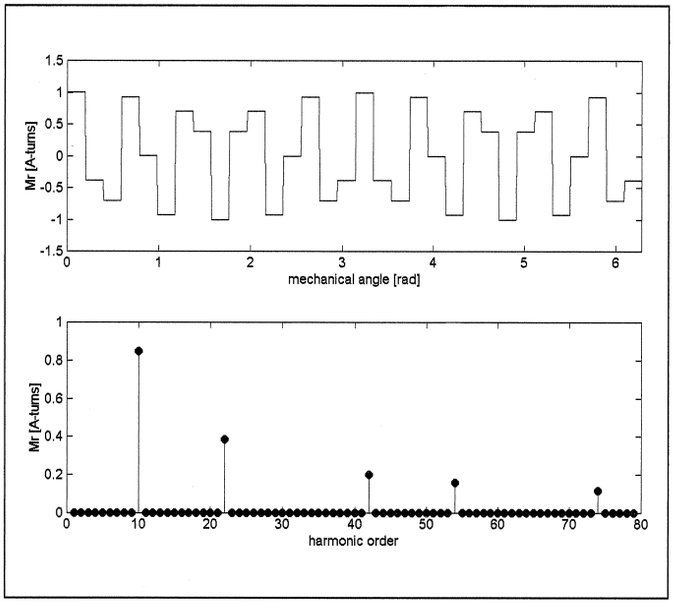

Figure 2. (a) Cage rotor MMF at an instant of time (p=2, R=32, m=(5) (top); (b) Spectral content of MMF from Figure 2(a) (bottom)

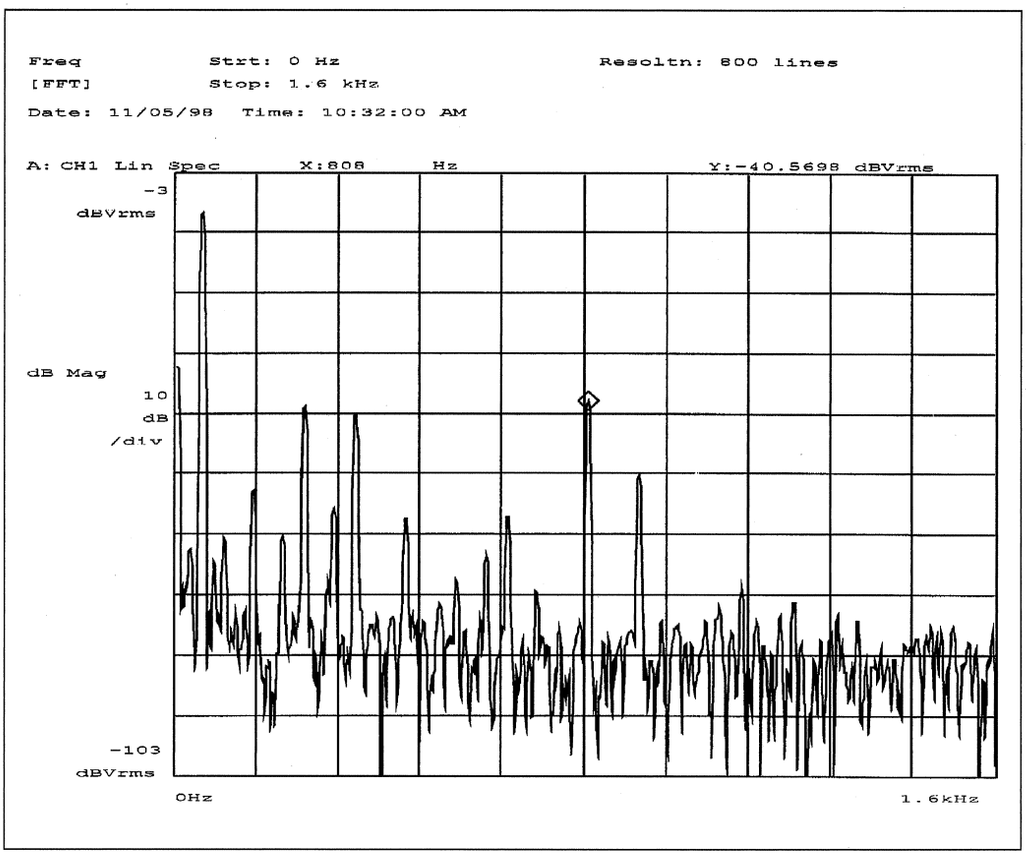

Figure 3. Stator current spectra for experimental motor (S=36, R=32, p=2, s=5.25%)

follows from (14) and (15) that the most significant impact on the stator emfs (currents) at discussed frequencies will have waves for which $\lambda R \pm \mu p = \pm p$ satisfied.

Figure 3 shows the stator current spectra for an experimental motor 3 kW, $p = 2$, with $S = 36$ and $R = 32$, stator winding connections Δ, at slip $s = 5.25\%$. S is the number of stator slots. The most prominent harmonic in the spectra is the higher rotor slot harmonic, at 808 Hz. In [4], Say points out that motors that fulfill the condition $S \pm R = 2p$ have very prominent rotor slot harmonics. The lower rotor slot harmonic at 708 Hz is of very small magnitude. The reason is the fact that lower rotor slot harmonic is triplen harmonic (from (14) follows for $s = 0$ and $\lambda = 1$: $|1 - R/p| = |1 - 32/2| = 15$) and since the stator winding is delta connected, the current of this frequency flows in delta.

The fact that all space harmonics from the stator side are reflected by cage rotor at only two frequencies (for $\lambda = 1$) is the main limiting factor for condition monitoring of various fault conditions such as interturn short circuits or static eccentricity condition of an induction machine [5]. Namely, in fault condition such as interturn short circuit in stator winding, all MMF and flux density space harmonics will appear in the air gap. But a cage rotor will reflect all of these harmonics at only two frequencies (for $\lambda = 1$) in stator current spectra, which exists in spectra even in a healthy machine.

Conclusions: As the result of the nature of the rotor cage winding, all MMF (flux density) space harmonics from the stator side will be reflected by the rotor at the fundamental frequency f_1 and at the frequencies $(1 \pm \lambda R(1-s)/p)f_1$. As a consequence, harmonic components will exist at these frequencies in the stator current spectra. The position of these components in the stator current spectra depends on actual rotor speed. This fact is employed for sensorless measurement of rotor speed. The fact that all space harmonics from the stator side are reflected by the cage rotor at only two frequencies (for $\lambda = 1$) is the main limiting factor for condition monitoring of various fault conditions of an induction machine such as interturn short circuits or static eccentricity conditions.

References:

[1] P. Vas, *Parameter Estimation, Condition Monitoring and Diagnosis of Electrical Machines. Monographs in Electrical and Electronic Engineering*. New York: Oxford Science Publications, 1993.

[2] K.D. Hurst and T.G. Habetler, "A comparison of spectrum estimation techniques for sensorless speed detection in induction machines," *IEEE Trans. Ind. Applicat.*, vol. 33, pp. 898-905, July/Aug. 1997.

[3] G. Joksimovic, M. Djurovic, and A. Obradovic, "Skew and linear rise of MMF across slot modeling-winding function approach," *IEEE Trans. Energy Conversion*, vol. 14, pp. 315-320, Sept. 1999.

[4] M..G. Say, *Alternating Current Machines*, 5th ed. New York: Pitman 1984.

[5] G. Joksimovic, "Analysis and simulation of faults in squirrel cage induction motors by multiple coupled circuit model," Ph.D. dissertation, University of Montenegro, Yugoslavia, 2000.

Manuscript received 10 March 2000; revised 18 September 2000. This paper is published herein in its entirety.

Application of Unified Power Flow Controller to Available Transfer Capability Enhancement

Y. Xiao, Y.H. Song, Y.Z. Sun

Author Affiliation: Brunel Institute of Power Systems (BIPS), Brunel University, Uxbridge, London UB8 3PH, U.K.; Tsinghua University, Beijing, China.

Abstract: From the point view of operational planning, a methodology for improving available transfer capability (ATC) by the unified power flow controller (UPFC) is presented. It is highly recognized that FACTS devices, especially the UPFC, can be applied to redistribute load sharing and support node voltage, therefore, to mitigate the critical situation that results from the increase of system loading or occurrence of inherent uncertainties in power systems. Thus, it is essential to take the impact of FACTS devices as an important issue for reinforcement of ATC. In this letter, with respect to the effect of UPFC, ATC is modeled as the maximum value of unused transfer power that causes no thermal or voltage limit violations. In the model formulated, three major uncertainties of power systems that affect the ATC value considerably are also considered. Case studies with a reduced practical system are presented. The technical merits of the UPFC for reinforcement of the ATC are demonstrated clearly.

Introduction: The requirement of the shared use of the existing network resources intensively and reliably have motivated the development of effective methods to enhance ATC. Various approaches have been proposed, such as the Lagrangian multiplier and the generalized reduced gradient method [3] and direct interior point algorithm [4]. Traditionally, rescheduling active power of generators, adjusting terminal voltage of generators, and taps changing of on-load tap changer (OLTC) are considered as major control variables for optimization. In a privatized electricity market, however, all of the parameters may not be centrally dispatched by the transmission network owner. On the other hand, in terms of steady-state power flow, since circuits do not normally share power in proportion to their ratings, and in most situations the voltage profile can not be smooth, ATC value will be limited ultimately by heavily loaded circuits and (or) nodes with relatively low voltage. Meanwhile, as stated, FACTS technology makes it possible to use circuit reactance, voltage magnitude, and angle as controls to redistribute line flow and regulate nodal voltage. Therefore, it can offer a convenient and promising alternative to conventional methods for the enhancement of ATC. Nevertheless, so far, from the view of operational planning, there are few reports about using FACTS to improve ATC of interconnected networks.

A new approach is proposed in this letter, which focuses on the application of the UPFC on transmission corridors to enhance ATC. To maintain the symmetry of the admittance matrix, the power injection model (PIM) is employed to derive control parameters of the UPFC(s). Furthermore, taking into consideration the main uncertainties of power systems associated with the determination of ATC value, a stochastic optimization model is formulated, thereby, providing more robust and practical information.

ATC Optimization Model Formulated: Based on PIM, which is shown in Figure 1, active and reactive power injections of the UPFC are taken as independent control variables for ATC optimization. For the

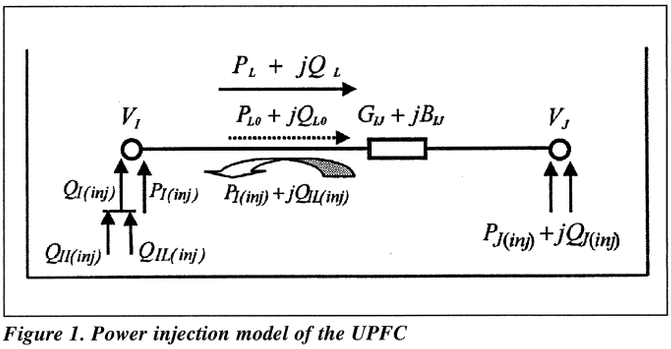

Figure 1. Power injection model of the UPFC